chemosensors

MDPI

Article

Electrochemically Prepared Unzipped Single Walled Carbon Nanotubes-MnO_2 Nanostructure Composites for Hydrogen Peroxide and Glucose Sensing

A. B. M. Zakaria [1,†] and Danuta Leszczynska [2,*]

[1] Department of Chemistry and Biochemistry, Jackson State University, Jackson, MS 39217, USA; abmzakaria@icnanotox.org

[2] Department of Civil and Environmental Engineering and Interdisciplinary Center of Nanotoxicity, Jackson State University, Jackson, MS 39217, USA

* Correspondence: danuta.leszczynska@jsums.edu; Tel.: +1-601-979-1091

† Current address: Department of Radiology and Biomedical Imaging, Yale School of Medicine, New Haven, CT 06520, USA.

Received: 14 November 2018; Accepted: 24 December 2018; Published: 3 January 2019

Abstract: Amperometric hydrogen peroxide (H_2O_2) and glucose biosensors based on unzipped carbon nanotubes with modified glassy carbon electrode (GCE) have been successfully fabricated via a facile electrochemical oxidative method. In this work, we investigated the feasibility of this new form of carbon nanomaterial as a substrate electrode material for fabricating sensitive platform for H_2O_2 and glucose sensors. For this purpose, the manganese oxide (MnO_2)/unzipped single-walled carbon nanotubes (SWCNTs) film was synthesized by the cyclic voltammetry method. The developed sensing film, MnO_2/unzipped SWCNTs/GCE, displayed a satisfactory analytical performance for H_2O_2, including a wide linear range of 2.0×10^{-6} to 5.0×10^{-3} M with a detection limit of 0.31×10^{-6} M (10.7 ppb). This film was further applied for glucose sensing with a linearity range of 0.01 to 1.2 mM with a correlation coefficient of 0.9822 in the physiological pH (7.4). This facile, fast, environmentally-friendly, and economical preparation strategy of carbon nanomaterial-based electrode materials opens up the possibility of developing high quality biocompatible hydrogen peroxide and glucose sensors.

Keywords: hydrogen peroxide sensor; glucose sensor; cyclic voltammetry; unzipped SWCNTs; electrochemical method

1. Introduction

Unzipped carbon nanotubes, a new transformed material commonly synthesized from carbon nanotubes (CNTs), are a combination of one-dimensional CNTs and two-dimensional graphene [1]. This unique nanostructure has also been called graphene nanoribbons (GNRs) [2,3]. It has attracted enormous interest from both theoretical and experimental scientists due to its unique electrical [4], optical [5], thermal [6], doping [7], magnetic [8], and mechanical [9] properties. To date, numerous experiments have been performed to categorize the practical significance in manufacturing devices, such as field-effect transistors [10], photodetectors [11], catalysts for proton exchange membrane (PEM) fuel cells [12], and magnetic field sensors [13]. However, very few reports have been published on using this carbon nanostructure as a substrate material for constructing sensors for specific measurements, such as hydrogen peroxide and glucose.

Various preparation methods for unzipping carbon nanotubes are known, such as plasma etching [14], annealing in hydrogen [15], intercalation–exfoliation [16], catalytic metal nanoparticle cutting [17], and chemical unzipping [18,19]. Among these methods, the electrochemical approach is

an effective way for converting carbon nanotubes (CNTs) to unzipped carbon nanotubes. Moreover, the electrochemical method has a unique advantage when compared with other methods, as it allows controlling of the layer's thickness and orientation [20–22]. Graphene-like unzipped carbon nanotubes consist of a sp^2 carbon plane, but have an elongated structure with a high aspect ratio, edge density, and defects sites, as well as high-quality graphene layers. These unique properties make them an excellent candidate for electrochemical sensing platforms with high current responses, and lower limits of detection towards target analytes.

Novel metal nanostructures incorporating carbon nanomaterials (CNMs) have shown great potential applications in the fields of electrochemical sensing devices. Recently, metal and transition metal oxide nanoparticles have been extensively applied in developing high efficient electrochemical sensing toward H_2O_2 and glucose [23–25]. Particularly, manganese oxide (MnO_2) nanoparticles are one of the most promising inorganic materials in fabricating sensing devices due to high catalytic ability, low-cost, high energy density, and environmental benignity [26–29].

Nowadays, H_2O_2 and glucose are suitable probe analytes to justify a new material in future biosensing applications. Several new forms of hybrid materials have been investigated by using these probe analytes. Most importantly, CNM-based sensors possess fast electron transfer kinetics, low limits of detection, and high sensitivity. For example, Yaojuan et al. investigated gold nanoparticle (AuNP)–graphene nanocomposites as a new electrode material synthesized by electrochemical deposition of Au–NPs on graphene sheets [30]. Selvakumar et al. demonstrated the glucose biosensing properties of a direct growth of glucose oxidase (GOx) on reduced graphene oxide/β-Cyclodextrin composite modified electrode for glucose monitoring [31]. Qinglin et al. fabricated glassy carbon electrode with graphene–carbon nanotube–nafion/gold–platinum alloy nanoparticles [32]. Nur et al. used Au nanoparticles supported graphene oxide nanoribbons (GONRs) [33]. Minmin et al. demonstrated Cu_2O nanocubes wrapped in graphene nanosheets (Cu_2O/GNs) as electrocatalysts [34]. Jasmina et al. reported an amperometric H_2O_2 sensor using a carbon paste electrode (CPE) coated with platinum nanoparticles on graphitized carbon (Pt–C) [35].

The preparation of these electrode materials is usually time-consuming and high-cost, and requires complicated, multi-step procedures. Therefore, a simple, low-cost preparation method to fabricate electrode is highly desired. In our previous work, we have achieved substantial progress on preparing substrate electrode material including synthesis and characterization of unzipped single-walled carbon nanotubes (unzipped SWCNTs) [36]. The obtained new form of carbon nanomaterial offers high active sites, fast electron transfer kinetics, and effective high surface area.

In this work, we report our extended study on preparing the final electrode material by the electrodeposition of MnO_2 on as-prepared unzipped SWCNTs modified glassy carbon electrode (GCE) and evaluating its electrocatalytic performances towards electrooxidation of the probe analytes, such as H_2O_2 and glucose.

2. Materials and Methods

2.1. Reagents and Apparatus

Single-walled carbon nanotubes (non-functionalized, purity >90 wt.%, outer diameter 1–2 nm, length 5–30 μm) were purchased from Cheap Tubes Inc. Cambridgeport, VT, USA. Nafion (perfluorinated ion-exchange resin), sulfuric acid (93–98 *w*/*w*%, density 1.84 g/cm^3 at 20 °C), $Na_2HPO_4{\cdot}7H2O$, KH_2PO_4, NaCl, KCl, glucose oxidase (from *Aspergillus niger*, 18,200 units g^{-1}), and glucose (D-(+)-99.5%) were purchased from Sigma-Aldrich (St. Louis, MO, USA). All chemicals were analytical grade and were used as received. All stock solutions were prepared using deionized water without further purification.

Amperometric and cyclic voltammograms were carried out with CH Instruments (CHI 440, CH Instruments, Austin, TX, USA) using a standard three-electrode system. The glassy carbon electrode (GCE), Ag/AgCl/saturated KCl (Model CH111, CH Instruments, Austin, TX, USA), and a

platinum wire were used as working, reference, and counter electrodes, respectively. High purity argon was used to deoxygenate all experimental solutions for 20 min, and maintaining argon atmosphere during experiments. Scanning electron microscopy (ZEISS Supra 40VP SEM) and transmission electron microscopy (JEOL-2100F operated at 100 kV) were used for characterizing the surface morphology and nanostructure of the carbon nanomaterials and MnO_2 nanoparticles.

2.2. Preparation of MnO_2/Unzipped SWCNTs/GCE

Unzipped SWCNTs/GCE was prepared as reported before [20,36]. Briefly, 5 mg of SWCNTs was dispersed in 5 mL of Nafion under 20 min constant ultrasonic agitations until obtaining 1 mg/mL of black homogeneous suspension. The glassy carbon electrode was polished with 0.05 µm alumina powder, and washed ultrasonically in deionized water and ethanol for 10 min. Then, a 3 µL of the black suspension was dropped onto cleaned GCE surface, and dried under a yellow lamp at 50 °C to obtain the SWCNTs/GCE.

The modified GCE was subjected to electrochemical oxidation in potential window of −0.2 to 0.7 V, at scan rate 100 mVs^{-1} in 0.5 M H_2SO_4 for 12 h. Then, MnO_2 was electrodeposited on the surface of unzipped SWCNTs/GCE by repetitive scanning cycles by applying potential window of 0.3 to 1.3 V in a solution of 0.1 M Na_2SO_4 and 5.0 mM $MnSO_4$. The electrochemical setup, including the steps of preparation method of modified glassy carbon electrode (GCE) and electrochemical reactions in sensing H_2O_2 and glucose, is illustrated in Figure 1.

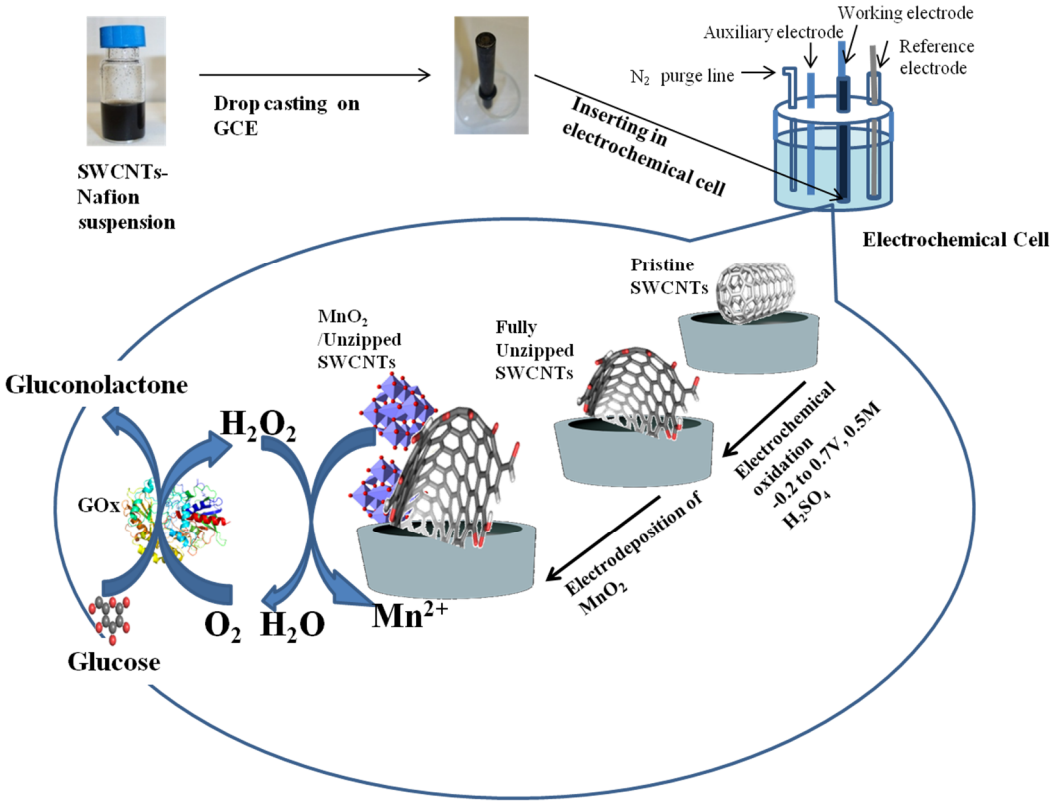

Figure 1. Schematic representation of the preparation of MnO_2/unzipped SWCNTs modified glassy carbon electrode (GCE) for glucose sensing.

3. Results and Discussion

3.1. Characterization of Unzipped SWCNTs and MnO_2 Nanostructured Film

The surface of SWCNTs was investigated before and after electrochemical treatment by scanning electron microscopy (SEM). Figure 2A shows the SEM image of the characteristic tubular networks

of pristine SWCNTs. After anodic oxidation, a cloudy surface morphology of CNT was observed (Figure 2B). This cloudy feature of unzipped SWCNTs was observed due to increasing edge carbon resulting hydrophilic nature developing on its surface and attaching atmospheric water molecules.

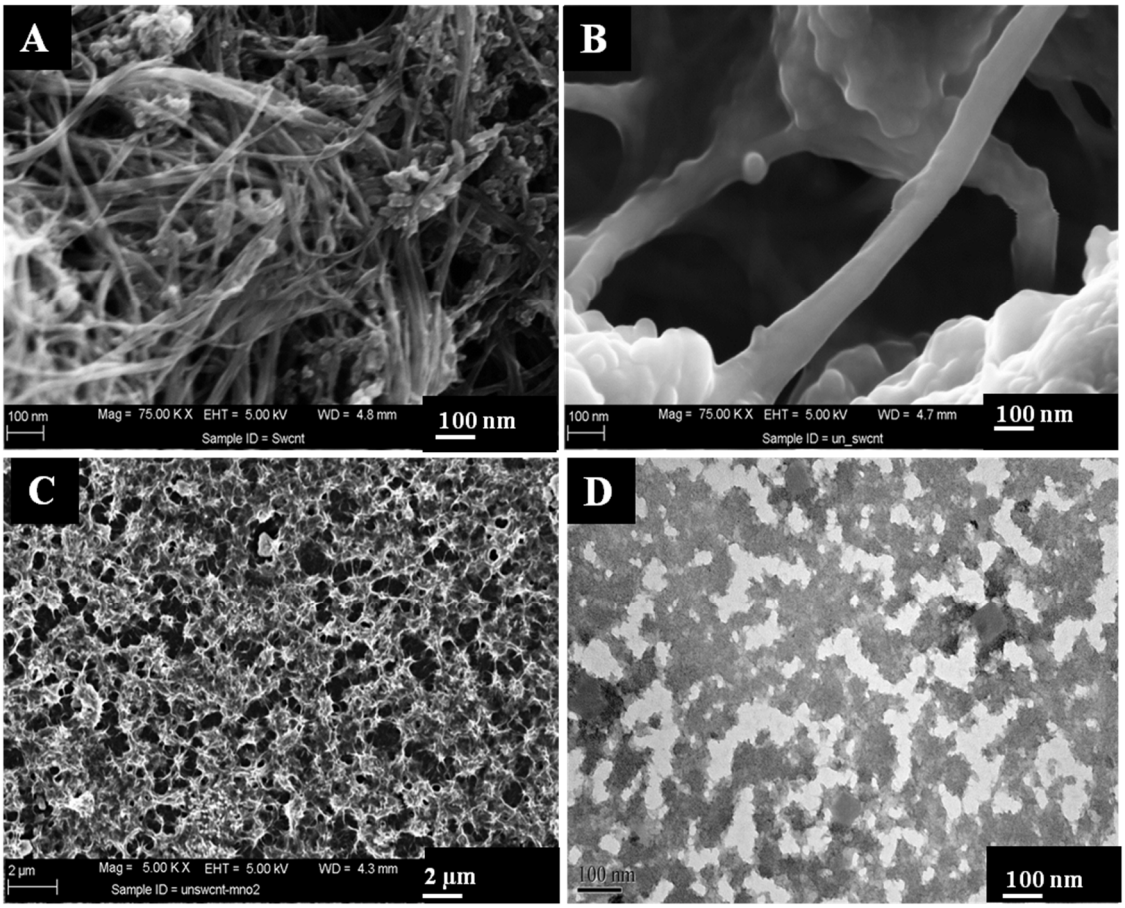

Figure 2. SEM images of pristine SWCNTs (**A**), unzipped SWCNTs (**B**), and spike like MnO_2 on unzipped SWCNTs (**C**). TEM image of MnO_2/unzipped SWCNTs (**D**).

In addition, Figure 2C,D depicts the spike-like MnO_2 anchored with edge carbon generated during transformation of SWCNTs to unzipped SWCNTs. The homogeneous structure of MnO_2/unzipped SWCNTs film suggests that MnO_2 was successfully attached on the surface of unzipped SWCNTs.

In order to confirm the oxidative opening (unzipping) of SWCNTs, we carried out Fourier transform infrared spectroscopy (FTIR) and Raman spectroscopy analyses. The FTIR (Figure 3A) spectrum of unzipped SWCNTs illustrates higher absorption of O–H group in the regions of O–H (3000–3700 cm^{-1}) and C=O modes (1700–1750 cm^{-1}), and lower absorption in the regions of C–O (1000–1250 cm^{-1}) and C=C–H (800–1000 cm^{-1}) compared to the spectrum of pristine SWCNTs. Moreover, Raman spectra (Figure 3B) also confirmed the fully unzipping of pristine SWCNTs. The G and D bands of SWCNTs has been reported as the characteristics of sp^2 carbon atoms and the extent of defects of carbon nanostructure respectively [37]. The spectrum of unzipped SWCNTs in Figure 3B shows the intensity of the D band at 1360 cm^{-1} and the G band at 1600 cm^{-1} s increased and broadened compared to the pristine SWCNTs. This observation is attributed to the confirmation of the formation of unzipped SWCNTs.

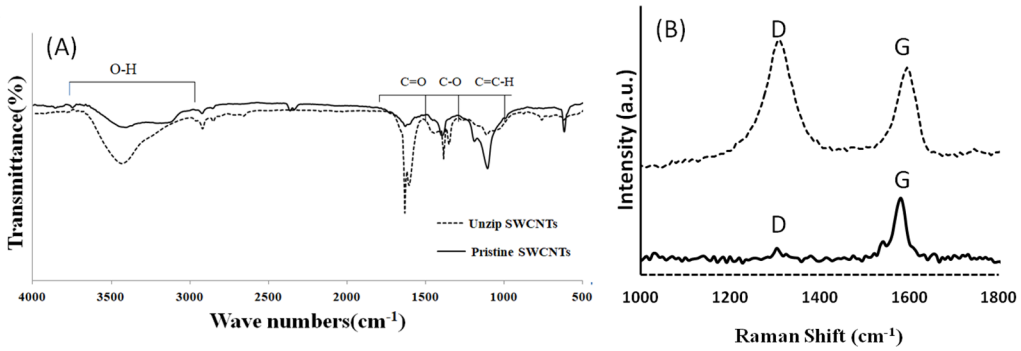

Figure 3. Comparisons of unzipped (—) and pristine (-) SWCNTs in (**A**) FTIR transmittance and (**B**) Raman spectra.

3.2. Formation of MnO_2 on Unzipped SWCNTs/GCE

Figure 4 shows the voltammograms of the first scan and scans after 12 h and 72 h, respectively, indicating the stable and successful unzipping of carbon nanotubes.

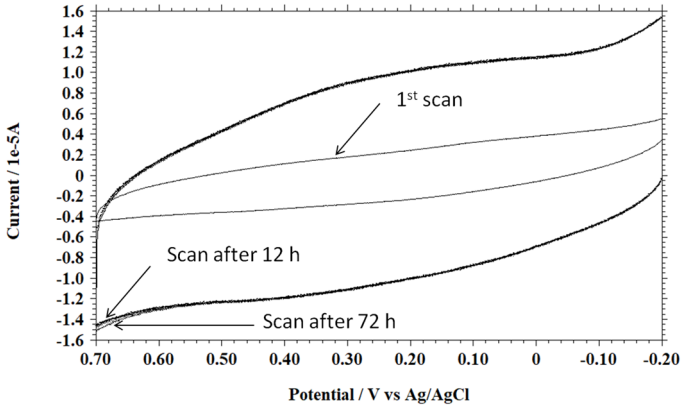

Figure 4. Cyclic voltammograms (oxidation) in 0.5 M H_2SO_4 at 100 mV s^{-1} scan rate in the potential window from −0.2 to 0.7 V vs. Ag/AgCl sat. KCl.

Figure 5A shows the cyclic voltammograms (CVs) obtained in solution of 0.1M Na_2SO_4 and 5.0 mM $MnSO_4$ at SWCNTs/GCE and unzipped SWCNTs/GCE. Obtained data strongly demonstrated that the sharp and large peak area of oxidizing Mn^{2+} to Mn^{3+} and reducing Mn^{3+} to Mn^{2+} was observed at unzipping SWCNTs when compared to pristine SWCNTs. The current intensity of oxidation and reduction during electrodeposition of MnO_2 was increased with repetitive voltammetric cycles (Figure 5B). This observation is consistent with our previous work [27]. It also suggests that large amounts of MnO_2 nanoparticles were successfully attached due to enlarged surface area with increasing active sites on unzipped SWCNTs.

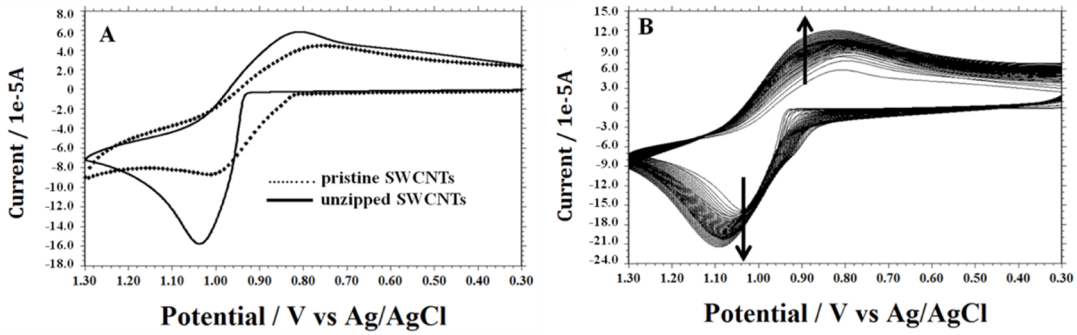

Figure 5. (**A**) Cyclic voltammograms (CVs) obtained at pristine SWCNTs and unzipped SWCNTs modified GC electrode in 0.1 M Na_2SO_4 containing 5.0 mM $MnSO_4$, at scan rate of 100 mV^{-1}; (**B**) electrodeposition of MnO_2 by repetitive CVs on unzipped SWCNTs/GCE.

3.3. Electrocatalytic Oxidation of H_2O_2 at MnO_2/Unzipped SWCNTs/GCE

Figure 6A displays the cyclic voltammetry (CV) obtained at the pristine SWCNTs/GCE (a), only MnO_2/GCE (b), unzipped SWCNTs/GCE (c), and MnO_2/unzipped SWCNTs/GCE (d) in 0.1 M PBS (pH 7.4) containing 1.0 mM H_2O_2, at a scan rate of 100 mVs^{-1}. The observed electrocatalytic ability of these different electrodes towards oxidation of H_2O_2 has shown following order: *MnO_2/unzipped SWCNTs/GCE > unzipped SWCNTs/GCE > MnO_2/GCE > Mn pristine SWCNTs/GCE*.

The pristine SWCNTs did not show any oxidation peak indicating its electrochemical inactivity in this potential window. The unzipped SWCNTs modified GCE showed some oxidation current due to available active sites generated during the opening of the side wall of the carbon nanotubes. In contrast, a noticeable oxidation peak at the potential of 0.85 V was observed at MnO_2/unzipped SWCNTs/GCE resulting from two factors. Firstly, MnO_2 has high catalytic activity for H_2O_2.

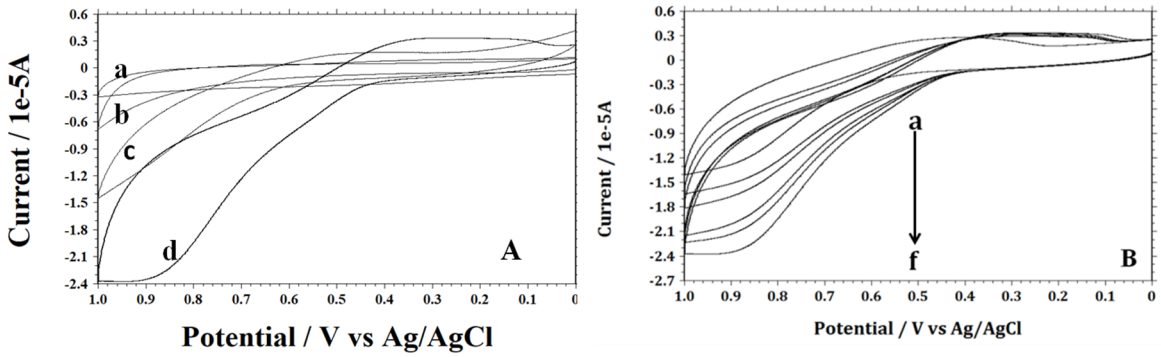

Figure 6. (**A**) Cyclic voltammograms (CVs) of different electrodes: (a) pristine SWCNTs, (b) only MnO_2, (c) unzipped SWCNTs, and (d) MnO_2/unzipped SWCNTs film modified GCE in presence of 1.0 mM of H_2O_2; (**B**) CVs of MnO_2/unzipped SWCNTs with different concentration of H_2O_2 (1.0 mM to 5.0 mM) in 0.1 M PBS (pH 7.4) at scan rate 100 mV/s.

Secondly, spike or edge-like structure of MnO_2 nanoparticles electrodeposited on unzipped SWCNTs might have higher catalytic ability for decomposing H_2O_2 than regular-sized nanoparticles. From Figure 6B, it is obvious that the oxidation peak current was proportional to increasing H_2O_2 concentration (a–f: 1.0 mM to 5.0 mM). The excellent electrochemical activity toward H_2O_2 can be attributed to the relatively high specific surface area, and the orientation of nanostructured MnO_2 on the unzipped SWCNTs/GCE surface.

3.4. Determination of H_2O_2

Figure 7 displays the amperometric current–time curve of MnO_2/unzipped SWCNTs/GCE for the successive addition of H_2O_2 in 0.1 M PBS (pH 7.4) at the potential +0.85 V. The figure (inset) also shows the calibration curve, and the regression equation of the sensor. The regression equation is as follows:

$$\boldsymbol{Ip(\mu A) = 0.0209x + 1.7781} \quad (1)$$

where $\boldsymbol{x}$ is the concentration of H_2O_2 in μM.

The linear range of this calibration curve was from 2.0×10^{-6} to 5.0×10^{-3} M with a correlation coefficient of 0.9831. From the slope of 0.0209 μA/μM, the limit of detection (LOD) was calculated to 0.31×10^{-6} M using the following equation:

$$\mathrm{LOD} = \mathrm{SD}_{\mathrm{background}}/\mathrm{S} \quad (2)$$

where S is slop or sensitivity, SD: Standard deviation.

The linearity range and sensitivity for detecting H_2O_2 at MnO_2/unzipped SWCNTs/GCE was greater than that of MnO_2/pristine SWCNTs/GCE, as was reported in our previous work [30]. In addition, the sensor exhibited appreciable reproducibility of 3.78% for five independent measurements carried out by five different MnO_2/unzipped SWCNT film modified electrodes.

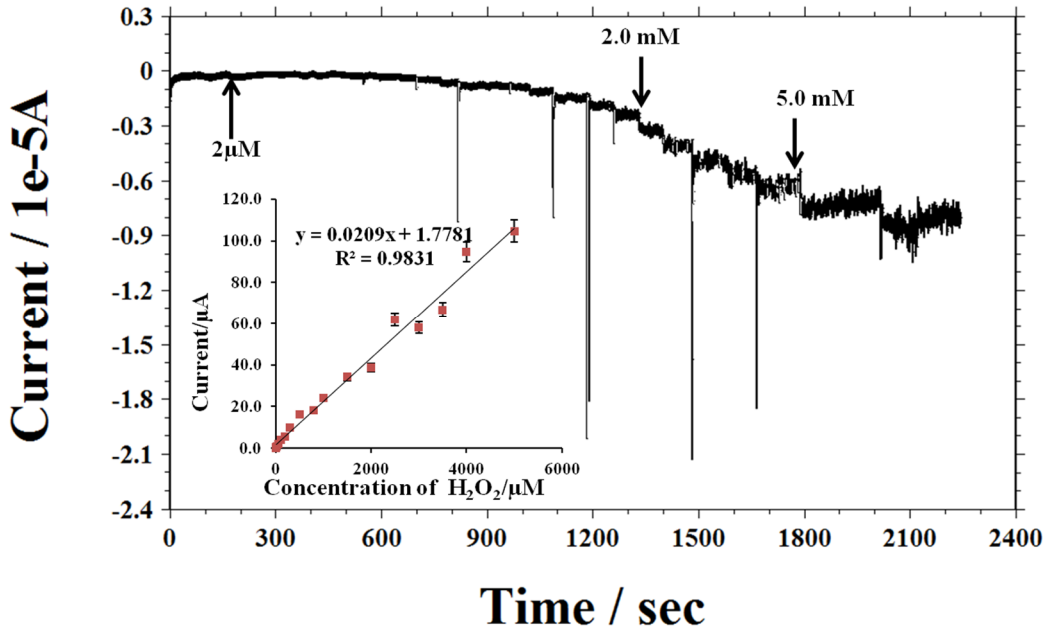

Figure 7. Current–time curve obtained on MnO_2/unzipped SWCNTs/GCE with successive addition of different concentration of H_2O_2 to 0.1 M, pH 7.4, PBS solution; inset: Calibration illustrating the linear relationship between electrode response to the concentration of H_2O_2.

Table 1 summarizes performance of different modified electrodes toward direct measurements of hydrogen peroxide in water matrix.

Table 1. Comparative performance of different composite electrodes for H_2O_2 detection.

Modified Electrode	Linear Range (mM)	Detection Limit (μM)	Reference
Pt NP/graphite-CS	0.25–2890 μM	66 nM	[35]
rGO/FeNPs/GCE	0.001–2.15	0.056	[28]
AgNPs/$Na_2Ti_3O_7$/Graphite	5.0–2500	1.0	[29]
MnO_2/CuO/GO NP/Cu wire	0.5–4.4	53.0	[38]
MnO_2/SWCNTs-Nf/GCE	0.005–3.0	0.52	Our previous work [27]
MnO_2/unzipped SWCNTs/GCE	0.002–5.0	0.3	**This work**

3.5. Application of MnO_2/Unzipped SWCNTs/GCE in Glucose Sensing

Glucose oxidase (GOx) was taken as the representative enzyme to investigate the electrocatalytic ability of MnO_2/unzipped SWCNTs modified GCE during glucose monitoring. As is well-known, glucose oxidase catalyzes the oxidation of glucose with oxygen, accompanying the production of gluconic acid and H_2O_2. Consequently, the concentration of glucose can be indirectly detected by the determination of the liberated H_2O_2 during the enzymatic catalysis. Figure 8 shows the amperometric response of the MnO_2/unzipped SWCNTs/GCE during successive addition of glucose to a solution containing 1 mg/1 mL GOx. Based on the current response towards the oxidation of H_2O_2 during the enzyme/glucose reaction, the calibration curve was plotted between catalytic current and glucose concentration. The linearity range was estimated from 0.01×10^{-3} to 1.2×10^{-3} M with a correlation coefficient of 0.9822 and the detection limit of the glucose was 1.2×10^{-6} M. Table 2 summarizes performance of several composite electrodes toward glucose detection, including our work.

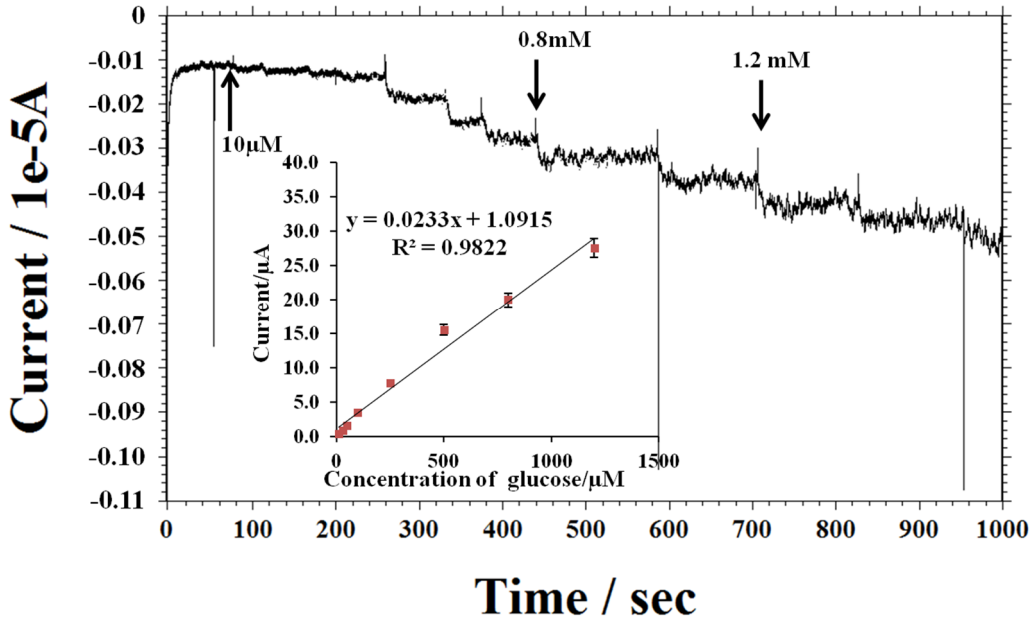

Figure 8. Current–time curve of MnO_2/unzipped SWCNTs/GCE with successive addition of glucose to 0.1 M, pH 7.4, PBS solution containing 1 mg/mL GOx at 0.85 V (vs. Ag/AgCl). Inset: Calibration illustrating the linear relationship between electrode responses to the glucose addition.

Table 2. Comparative performance of different composite electrodes for glucose detection.

Modified Electrode	Linear Range (mM)	Detection Limit (μM)	Reference
Mn_3O_4 NP/3D GF	0.1–8	10	[39]
SnO_2 NP/rGO/GCE	0.05–5.00	13.35	[40]
Mn-Cu NP/MWCNT/GCE	1–32	1.0	[41]
MnO_2/CuO/GO NP/Cu wire	0.5–4.4	53	[38]
GOx/rGO/CD/GCE	0.050–3.0	12	[31]
MnO_2/unzipped SWCNTs/GC	0.01–1.2	1.2	**This work**

3.6. Selectivity, Stability and Reproducibility Property of the MnO_2/Unzipped SWCNTs/GCE

The prepared electrode showed higher stability for amperometric measurement at a constant potential. Figure 9A displays the stability response without addition of glucose to 0.1 M, pH 7.4, PBS solution containing 1 mg/mL GOx at 0.85 V (vs. Ag/AgCl). The reproducibility of the as-prepared electrode was also evaluated by measuring amperometric (E_{ap} = 0.85 V) responses of the sequential addition of 0.1 mM of glucose in 0.1M PBS. The relative standard deviation (R.S.D) was 5.4% suggesting the high reproducibility of the prepared electrode. Moreover, Figure 9B shows the amperometric response of the sequential addition of 0.1 mM glucose, and the common interferents including uric acid (UA) and ascorbic acid (AA) of 0.1 mM for each addition. The significant response for glucose and insignificant responses for interfering species were observed, suggesting good selectivity for glucose detection.

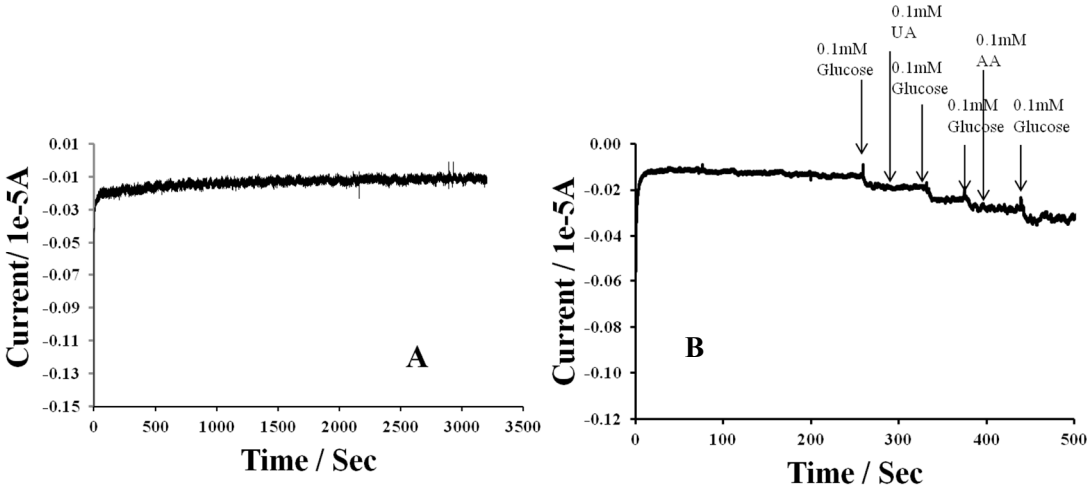

Figure 9. (**A**) Current–time curve of MnO_2/Unzipped SWCNTs/GCE electrode in absence of glucose over 3000 s and (**B**) the sequential addition of 0.1 mM glucose, 0.1 mM UA and 0.1 mM AA 0.1 M, pH 7.4, PBS solution containing 1 mg/mL GOx at 0.85 V (vs. Ag/AgCl).

4. Conclusions

We have outlined a facile methodology for constructing a suitable electrochemical sensing platform based on MnO_2/unzipped SWCNTs that exhibits high electrocatalytic activity toward the oxidation of H_2O_2 in physiological pH of 7.4. Electrochemical method presents an efficient approach for tunable, simple and fast preparation of MnO_2/unzipped SWCNTs film. More importantly, electrochemically synthesized unzipped SWCNTs provided sufficient anchoring sites that allowed the formation of high electrocatalytic MnO_2 nanostructured film. Consequently, the as-prepared MnO_2/unzipped SWCNTs can be used for monitoring H_2O_2 at a low potential of 0.85 V with high sensitivity. The estimated linearity range for measuring H_2O_2 was found to be from 2.0×10^{-6} to 5.0×10^{-3} M and the detection limit was 0.31×10^{-6} M. Furthermore, this modified electrode was detecting very low concentration (1.2×10^{-6} M) of glucose. The results show that MnO_2/unzipped

SWCNTs are good nanostructured materials that can be applied for developing biosensors for monitoring different biological analytes.

Author Contributions: There is a balanced contribution to this study from two co-authors; Conceptualization, A.B.M.Z. and D.L.; Investigation, A.B.M.Z. and D.L.; Supervision, D.L.; Writing—original draft, A.B.M.Z.; Writing—review & editing, D.L.

Funding: This study was financially supported by the National Science Foundation (grants: EPS-362492-190200-01; EPS-0903787; and HRD 1547754; RCMI-8G12MD007581).

Acknowledgments: The authors would like to offer special thanks to Hiroyasu Tachikawa for using his electrochemical workstation.

Conflicts of Interest: The authors declare no conflict of interest.

References

1. Kim, N.D.; Li, Y.; Wang, G.; Fan, X.; Jiang, J.; Li, L.; Ji, Y.; Ruan, G.; Hauge, R.H.; Tour, J.M. Growth and Transfer of Seamless 3D Graphene–Nanotube Hybrids. *Nano Lett.* **2016**, *16*, 1287–1292. [CrossRef] [PubMed]
2. Kosynkin, D.V.; Higginbotham, A.L.; Sinitskii, A.; Lomeda, J.R.; Dimiev, A.; Price, B.K.; Tour, J.M. Longitudinal unzipping of carbon nanotubes to form graphene nanoribbons. *Nature* **2009**, *458*, 872–876. [CrossRef] [PubMed]
3. John, R.; Shinde, D.B.; Liu, L.; Ding, F.; Xu, Z.; Vijayan, C.; Pillai, V.K.; Pradeep, T. Sequential Electrochemical Unzipping of Single-Walled Carbon Nanotubes to Graphene Ribbons Revealed by in Situ Raman Spectroscopy and Imaging. *ACS Nano* **2014**, *8*, 234–242. [CrossRef] [PubMed]
4. Li, Y.; Zhou, W.; Wang, H.; Xie, L.; Liang, Y.; Wei, F.; Idrobo, J.-C.; Pennycook, S.J.; Dai, H. An oxygen reduction electrocatalyst based on carbon nanotube-graphene complexes. *Nat. Nano* **2012**, *7*, 394–400. [CrossRef] [PubMed]
5. Deilmann, T.; Rohlfing, M. Huge Trionic Effects in Graphene Nanoribbons. *Nano Lett.* **2017**, *17*, 6833–6837. [CrossRef]
6. Chen, X.; Xu, Y.; Zou, X.; Gu, B.-L.; Duan, W. Interfacial thermal conductance of partially unzipped carbon nanotubes: Linear scaling and exponential decay. *Phys. Rev. B* **2013**, *87*, 155438. [CrossRef]
7. Ervasti, M.M.; Fan, Z.; Uppstu, A.; Krasheninnikov, A.V.; Harju, A. Silicon and silicon-nitrogen impurities in graphene: Structure, energetics, and effects on electronic transport. *Phys. Rev. B* **2015**, *92*, 235412. [CrossRef]
8. Chen, X.; Zhang, L.; Guo, H. Valley caloritronics and its realization by graphene nanoribbons. *Phys. Rev. B* **2015**, *92*, 155427. [CrossRef]
9. Yan, Z.; Peng, Z.; Casillas, G.; Lin, J.; Xiang, C.; Zhou, H.; Yang, Y.; Ruan, G.; Raji, A.-R.O.; Samuel, E.L.G.; et al. Rebar Graphene. *ACS Nano* **2014**, *8*, 5061–5068. [CrossRef]
10. Candini, A.; Martini, L.; Chen, Z.; Mishra, N.; Convertino, D.; Coletti, C.; Narita, A.; Feng, X.; Müllen, K.; Affronte, M. High Photoresponsivity in Graphene Nanoribbon Field-Effect Transistor Devices Contacted with Graphene Electrodes. *J. Phys. Chem. C* **2017**, *121*, 10620–10625. [CrossRef]
11. Wei, D.; Xie, L.; Lee, K.K.; Hu, Z.; Tan, S.; Chen, W.; Sow, C.H.; Chen, K.; Liu, Y.; Wee, A.T.S. Controllable unzipping for intramolecular junctions of graphene nanoribbons and single-walled carbon nanotubes. *Nat. Commun.* **2013**, *4*, 1374. [CrossRef]
12. Long, D.; Li, W.; Qiao, W.; Miyawaki, J.; Yoon, S.-H.; Mochida, I.; Ling, L. Partially unzipped carbon nanotubes as a superior catalyst support for PEM fuel cells. *Chem. Commun.* **2011**, *47*, 9429–9431. [CrossRef] [PubMed]
13. Costamagna, S.; Schulz, A.; Covaci, L.; Peeters, F. Partially unzipped carbon nanotubes as magnetic field sensors. *Appl. Phys. Lett.* **2012**, *100*, 232104. [CrossRef]
14. Jiao, L.; Zhang, L.; Wang, X.; Diankov, G.; Dai, H. Narrow graphene nanoribbons from carbon nanotubes. *Nature* **2009**, *458*, 877–880. [CrossRef] [PubMed]
15. Talyzin, A.V.; Luzan, S.; Anoshkin, I.V.; Nasibulin, A.G.; Jiang, H.; Kauppinen, E.I.; Mikoushkin, V.M.; Shnitov, V.V.; Marchenko, D.E.; Noréus, D. Hydrogenation, Purification, and Unzipping of Carbon Nanotubes by Reaction with Molecular Hydrogen: Road to Graphane Nanoribbons. *ACS Nano* **2011**, *5*, 5132–5140. [CrossRef] [PubMed]

16. Kosynkin, D.V.; Lu, W.; Sinitskii, A.; Pera, G.; Sun, Z.; Tour, J.M. Highly Conductive Graphene Nanoribbons by Longitudinal Splitting of Carbon Nanotubes Using Potassium Vapor. *ACS Nano* **2011**, *5*, 968–974. [CrossRef] [PubMed]
17. Elías, A.L.; Botello-Méndez, A.R.; Meneses-Rodríguez, D.; Jehová González, V.; Ramírez-González, D.; Ci, L.; Munoz-Sandoval, E.; Ajayan, P.M.; Terrones, H.; Terrones, M. Longitudinal cutting of pure and doped carbon nanotubes to form graphitic nanoribbons using metal clusters as nanoscalpels. *Nano Lett.* **2009**, *10*, 366–372. [CrossRef]
18. Jiao, L.; Wang, X.; Diankov, G.; Wang, H.; Dai, H. Facile synthesis of high-quality graphene nanoribbons. *Nat. Nanotechnol.* **2010**, *5*, 321–325. [CrossRef]
19. Zehtab Yazdi, A.; Chizari, K.; Jalilov, A.S.; Tour, J.; Sundararaj, U. Helical and Dendritic Unzipping of Carbon Nanotubes: A Route to Nitrogen-Doped Graphene Nanoribbons. *ACS Nano* **2015**, *9*, 5833–5845. [CrossRef]
20. Shinde, D.B.; Debgupta, J.; Kushwaha, A.; Aslam, M.; Pillai, V.K. Electrochemical Unzipping of Multi-walled Carbon Nanotubes for Facile Synthesis of High-Quality Graphene Nanoribbons. *J. Am. Chem. Soc.* **2011**, *133*, 4168–4171. [CrossRef]
21. Guo, H.-L.; Wang, X.-F.; Qian, Q.-Y.; Wang, F.-B.; Xia, X.-H. A Green Approach to the Synthesis of Graphene Nanosheets. *ACS Nano* **2009**, *3*, 2653–2659. [CrossRef] [PubMed]
22. Zakaria, A.B.M.; Vasquez, E.S.; Walters, K.B.; Leszczynska, D. Functional holey graphene oxide: A new electrochemically transformed substrate material for dopamine sensing. *RSC Adv.* **2015**, *5*, 107123–107135. [CrossRef]
23. Palanisamy, S.; Cheemalapati, S.; Chen, S.-M. Amperometric glucose biosensor based on glucose oxidase dispersed in multiwalled carbon nanotubes/graphene oxide hybrid biocomposite. *Mater. Sci. Eng. C* **2014**, *34*, 207–213. [CrossRef] [PubMed]
24. Unnikrishnan, B.; Palanisamy, S.; Chen, S.-M. A simple electrochemical approach to fabricate a glucose biosensor based on graphene–glucose oxidase biocomposite. *Biosens. Bioelectron.* **2013**, *39*, 70–75. [CrossRef] [PubMed]
25. Palanisamy, S.; Chen, S.-M.; Sarawathi, R. A novel nonenzymatic hydrogen peroxide sensor based on reduced graphene oxide/ZnO composite modified electrode. *Sens. Actuators B Chem.* **2012**, *166–167*, 372–377. [CrossRef]
26. Han, Y.; Zheng, J.; Dong, S. A novel nonenzymatic hydrogen peroxide sensor based on Ag–MnO_2–MWCNTs nanocomposites. *Electrochim. Acta* **2013**, *90*, 35–43. [CrossRef]
27. Zakaria, A.; Leszczynska, D. Novel design of non-enzymatic sensor for rapid monitoring of hydrogen peroxide in water matrix. *J. Electroanal. Chem.* **2016**, *766*, 30–36. [CrossRef]
28. Vukojević, V.; Djurdjić, S.; Ognjanović, M.; Fabián, M.; Samphao, A.; Kalcher, K.; Stanković, D.M. Enzymatic glucose biosensor based on manganese dioxide nanoparticles decorated on graphene nanoribbons. *J. Electroanal. Chem.* **2018**, *823*, 610–616. [CrossRef]
29. Schachl, K.; Alemu, H.; Kalcher, K.; Moderegger, H.; Svancara, I.; Vytras, K. Amperometric determination of hydrogen peroxide with a manganese dioxide film-modified screen printed carbon electrode. *Fresenius J. Anal. Chem.* **1998**, *362*, 194–200. [CrossRef]
30. Hu, Y.; Jin, J.; Wu, P.; Zhang, H.; Cai, C. Graphene–gold nanostructure composites fabricated by electrodeposition and their electrocatalytic activity toward the oxygen reduction and glucose oxidation. *Electrochim. Acta* **2010**, *56*, 491–500. [CrossRef]
31. Palanisamy, S.; Devasenathipathy, R.; Chen, S.-M.; Ajmal Ali, M.; Karuppiah, C.; Balakumar, V.; Prakash, P.; Elshikh, M.S.; Al-Hemaid, F.M.A. Direct Electrochemistry of Glucose Oxidase at Reduced Graphene Oxide and β-Cyclodextrin Composite Modified Electrode and Application for Glucose Biosensing. *Electroanalysis* **2015**, *27*, 2412–2420. [CrossRef]
32. Sheng, Q.; Wang, M.; Zheng, J. A novel hydrogen peroxide biosensor based on enzymatically induced deposition of polyaniline on the functionalized graphene–carbon nanotube hybrid materials. *Sens. Actuators B Chem.* **2011**, *160*, 1070–1077. [CrossRef]
33. Ismail, N.S.; Le, Q.H.; Yoshikawa, H.; Saito, M.; Tamiya, E. Development of Non-enzymatic Electrochemical Glucose Sensor Based on Graphene Oxide Nanoribbon—Gold Nanoparticle Hybrid. *Electrochim. Acta* **2014**, *146*, 98–105. [CrossRef]

34. Liu, M.; Liu, R.; Chen, W. Graphene wrapped Cu_2O nanocubes: Non-enzymatic electrochemical sensors for the detection of glucose and hydrogen peroxide with enhanced stability. *Biosens. Bioelectron.* **2013**, *45*, 206–212. [CrossRef] [PubMed]
35. Anojčić, J.; Guzsvány, V.; Vajdle, O.; Kónya, Z.; Kalcher, K. Rapid amperometric determination of H_2O_2 by a Pt nanoparticle/Vulcan XC72 composite-coated carbon paste electrode in disinfection and contact lens solutions. *Monatshefte Chem. Chem. Mon.* **2018**, *149*, 1727–1738. [CrossRef]
36. Zakaria, A.; Leszczynska, D.; Novikov, V. (Eds.) A Facial Electrochemical Method for Preparation and Characterization of Graphene Nanoribbons from Single Walled Carbon Nanotubes. In *Mordern Directions in Chemistry, Biology, Pharmacy and Biotechnology*; Lviv Polytechnic Publishing House: Lviv, Ukraine, 2015; pp. 110–116.
37. Dresselhaus, M.S.; Dresselhaus, G.; Jorio, A.; Souza Filho, A.G.; Saito, R. Raman spectroscopy on isolated single wall carbon nanotubes. *Carbon* **2002**, *40*, 2043–2061. [CrossRef]
38. Farid, M.M.; Goudini, L.; Piri, F.; Zamani, A.; Saadati, F. Molecular imprinting method for fabricating novel glucose sensor: Polyvinyl acetate electrode reinforced by MnO_2/CuO loaded on graphene oxide nanoparticles. *Food Chem.* **2016**, *194*, 61–67. [CrossRef] [PubMed]
39. Si, P.; Dong, X.-C.; Chen, P.; Kim, D.-H. A hierarchically structured composite of Mn_3O_4/3D graphene foam for flexible nonenzymatic biosensors. *J. Mater. Chem. B* **2013**, *1*, 110–115. [CrossRef]
40. Ye, Y.; Wang, P.; Dai, E.; Liu, J.; Tian, Z.; Liang, C.; Shao, G. A novel reduction approach to fabricate quantum-sized SnO_2-conjugated reduced graphene oxide nanocomposites as non-enzymatic glucose sensors. *Phys. Chem. Chem. Phys.* **2014**, *16*, 8801–8807. [CrossRef]
41. Lin, K.-C.; Huang, L.-H.; Chen, S.-M. Electrochemical synthesis of mixed-valence manganese/copper hybrid composite using graphene oxide and multi-walled carbon nanotubes for nonenzymatic glucose sensor. *J. Electroanal. Chem.* **2014**, *735*, 36–42. [CrossRef]